

Factors That Limit Positron Emission Tomography Imaging of P-Glycoprotein Density at the Blood–Brain Barrier

Pavitra Kannan,^{†,‡} Victor W. Pike,[†] Christer Halldin,[‡] Oliver Langer,^{§,||} Michael M. Gottesman,[⊥] Robert B. Innis,^{*,†} and Matthew D. Hall[⊥]

[†]Molecular Imaging Branch, National Institute of Mental Health, National Institutes of Health, Bethesda, Maryland 20892, United States

[‡]Department of Clinical Neuroscience, Karolinska Institutet, 17176 Stockholm, Sweden

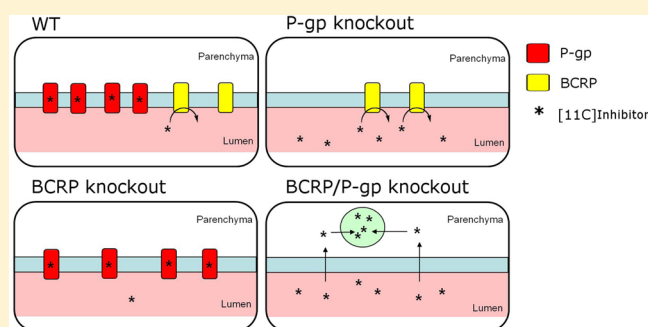
[§]Health and Environment Department, Biomedical Systems, AIT Austrian Institute of Technology GmbH, 2444 Seibersdorf, Austria

^{||}Department of Clinical Pharmacology, Medical University of Vienna, 1090 Vienna, Austria

[⊥]Laboratory of Cell Biology, National Cancer Institute, National Institutes of Health, Bethesda, Maryland 20892, United States

ABSTRACT: Efflux transporters located at the blood–brain barrier, such as P-glycoprotein (P-gp) and breast cancer resistance protein (BCRP), regulate the passage of many drugs in and out of the brain. Changes in the function and density of these proteins, in particular P-gp, may play a role in several neurological disorders. Several radioligands have been developed for measuring P-gp function at the blood–brain barrier of human subjects with positron emission tomography (PET). However, attempts to measure P-gp density with radiolabeled inhibitors that bind to these proteins *in vivo* have not thus far provided useful, quantifiable PET signals. Herein, we argue that not only the low density of transporters in the brain as a whole but also their very high density in brain capillaries act to lower the concentration of ligand in the plasma and thereby contribute to absent or low signals in PET studies of P-gp density. Our calculations, based on published data and theoretical approximations, estimate that whole brain densities of many efflux transporters at the blood–brain barrier range from 0.04 to 5.19 nM. We conclude that the moderate affinities (>5 nM) of currently labeled inhibitors may not allow measurement of efflux transporter density at the blood–brain barrier, and inhibitors with substantially higher affinity will be needed for density imaging of P-gp and other blood–brain barrier transporters.

KEYWORDS: positron emission tomography (PET), ABC transporters, imaging, blood–brain barrier, inhibitors, density



INTRODUCTION

P-Glycoprotein (P-gp, encoded by *ABCB1*) and breast cancer resistance protein (BCRP, encoded by *ABCG2*) are among the efflux transporters that are essential to the function of the blood–brain barrier.¹ These two transporters are apically located (blood-facing) in the endothelial cells of brain capillaries to prevent the entry of drugs into the brain, thereby protecting it from exposure to toxins in the blood.^{2,3} As a result, P-gp and BCRP can also impede the entry of potential therapeutics to the brain, and this barrier function may be exacerbated in pathophysiological conditions. Increased function of P-gp, for example, may contribute to drug resistance in epilepsy and may decrease the effectiveness of treating HIV infection of the brain.^{4,5} Changes in expression (i.e., density) of these transporters may also be clinically relevant because expression affects efflux capacity. For example, loss of P-gp expression would result in net decrease in function and, consequently, in dysfunction of the blood–brain barrier. Because the function and density of P-gp and BCRP in neurological disorders are not well understood

in vivo, quantifying both transporter function and density is a significant and important challenge.

Molecular imaging techniques such as positron emission tomography (PET) offer the potential for *in vivo* measurement of function and density of protein targets. In PET, a radiotracer is injected at a subpharmacological dose, and biomathematical modeling is applied to acquired data to determine output measures related to the interaction of the radiotracer with the receptor target. In the case of functional studies, increased or decreased uptake of a radiotracer measures protein function. Glucose metabolism in tissue, for example, is reflected by increased uptake of [¹⁸F]fluorodeoxyglucose.⁶ Efflux transport by P-gp or BCRP, on the other hand, is reflected by little to no uptake of the radiolabeled substrate in tissue, and inhibition of efflux transport results in increased substrate accumulation.¹ PET

Received: January 8, 2013

Revised: March 27, 2013

Accepted: April 18, 2013

Published: April 18, 2013

Table 1. Brain Concentrations of Radiolabeled P-gp and BCRP Inhibitors in Rat and Mouse Measured 30 min after Injection

radiolabeled inhibitor	radiotracer uptake in rat brain at 25 min			radiotracer uptake in mouse brain at 30 min					reference
	baseline	blocked	unit ^a	wild-type	P-gp knockout	BCRP knockout	P-gp/BCRP knockout	unit	
[¹¹ C]laniquidar	0.07	0.6	%ID/g						18
[¹¹ C]elacridar				0.05	0.15	0.05	1.0	SUV	22
	0.20	1.08	SUV	0.18	0.46	0.20	1.39	SUV	16
1-[¹⁸ F]fluoroelacridar	0.14	1.29	SUV	0.23			1.76	SUV	17
[¹⁸ F]fluoroethylacridar				0.08	0.18	0.08	0.70	SUV	21
[¹¹ C]tariquidar				0.02	0.04	0.02	0.75	SUV	20
	0.19	0.54	SUV	0.15	0.31	0.18	1.39	SUV	15
[¹⁸ F]fluoroethyltariquidar				0.07	0.14	0.10	0.60	SUV	21
[¹¹ C]-1 ^b	1.2	0.90	SUV						19
[¹¹ C]-2 ^c				0.96	1.17	0.80	1.79	SUV	23

^a%ID/g = % injected dose/gram of tissue. SUV = standardized uptake value, which is the ratio of radioactivity concentration measured in tissue at time *t* to injected dose at time of injection divided by body weight. A SUV of 1.0 is the value that would be obtained throughout the body for a hypothetical perfectly uniform distribution. ^b1 = novel P-gp inhibitor, [¹¹C]6,7-dimethoxy-2-{3-[4-methoxy-3,4-dihydro-2*H* naphthalene-(1*E*)-ylidene]-propyl}-1,2,3,4-tetrahydro-isoquinoline ^c2 = putative BCRP inhibitor, [¹¹C]methyl 4-((4-(2-(6,7-dimethoxy-1,2,3,4-tetrahydroisoquinolin-2-yl)ethyl)phenyl)amino-carbonyl)-2-(quinoline-2-carbonylamino)benzoate

has been successful in using radiolabeled substrates to measure P-gp function at the blood–brain barrier for at least two reasons. First, each molecule of P-gp can transport multiple substrate molecules. Second, upon inhibition of transport, amplification of the PET signal can occur by trapping some of the substrate in cellular organelles.^{7,8}

In the case of density studies, the density of the target is inferred from the binding potential—a parameter that is the product of the concentration of binding sites (B_{max}) and the affinity of the radioligand for the protein ($1/K_D$, where K_D is the equilibrium dissociation constant).⁹ [The term radioligand describes a specific class of compounds that reversibly or irreversibly bind to the protein target (e.g., radiolabeled inhibitor), whereas the term radiotracer refers to a more general class of compounds that includes substrates and radioligands.] Because substrates are transported quickly when in the vicinity of a transporter,¹⁰ they cannot be used to measure the density of these efflux transporters by PET. Inhibitors of P-gp or of BCRP, on the other hand, are known to directly bind to their respective transporters¹⁰ and might behave akin to antagonist receptor radioligands, thereby measuring density. However, PET has been unsuccessful at measuring P-gp density using radiolabeled inhibitors. Unlike the signal amplification obtained by substrate trapping, the maximal signal that can be obtained by binding is one radiolabeled inhibitor for each transporter (assuming one binding site per transporter). The difficulty in imaging P-gp density is also due to two previously described phenomena. First, many of the inhibitors cross-react with P-gp and BCRP,¹¹ which confounds results obtained in P-gp knockout, Bcrp knockout, or P-gp/Bcrp knockout mice. Second, some inhibitors of P-gp are also substrates for BCRP.¹² At very low concentrations, high affinity inhibitors might be transported by P-gp, but evidence for this appears to be conflicting.^{13,14}

The purpose of this perspective is to highlight two other difficulties of imaging P-gp density at the blood–brain barrier using PET. The first is that the density of P-gp in the whole brain has been variably reported in the literature but plays a critical role in the affinity of the radioligand required to have a measurable signal from *in vivo* PET imaging. This may be exacerbated by the low resolution of PET imaging. The second difficulty, which has not been discussed in the literature, is the high density of P-gp within the local microenvironment (microcompartment) of the

capillary. We propose that the density of P-gp (and BCRP) is high enough within the capillary compartment to substantially affect the free concentration of radiotracer during its 1–2 s transit through the capillaries. Here, we use the results from PET studies of P-gp density to explain how these two factors—low binding potential and high, localized transporter density—may greatly affect brain signal.

In the following sections, we assume for simplicity that: (1) The brain signal measured in PET studies of P-gp density is “binding to P-gp”. In reality, “brain uptake of radioactivity” includes both parenchymal uptake (after passing the blood–brain barrier) and radioactivity in the vascular compartment (about 5% of total brain volume (see below)). PET studies seek to determine the amount of radiolabeled inhibitor bound to P-gp in the brain capillaries. However, PET lacks the resolution to separately measure uptake in parenchyma and that in the vascular compartment. (2) A radiolabeled inhibitor can bind to all the P-gp in brain endothelial cells, but the majority of P-gp is localized at the luminal membrane. While P-gp is constantly recycled on/off the cell surface, the majority is thought to be expressed at the cell surface.

■ RESULTS FROM PET STUDIES MEASURING P-GP DENSITY

PET studies using high-affinity P-gp/BCRP inhibitors to measure transporter density at the blood–brain barrier have yielded confusing results (Table 1). According to conventional PET studies measuring receptor density, the specific binding of a radioligand to its receptor should be displaceable.⁹ If we assume that a radiolabeled inhibitor binds only to P-gp (i.e., is specific), then high concentrations of unlabeled inhibitor should displace the radioligand bound to P-gp and consequently decrease the measured brain signal. However, brain uptake of all except one of the tested radiolabeled inhibitors was low 30 min after injection in wild-type rats but *increased* at least 150% after blockade with high doses of nonradiolabeled inhibitors; the increase was not due to altered peripheral metabolism after blockade.^{15–19} Results obtained from transgenic mice are also not consistent with expectations for a P-gp binding molecule. For example, brain uptake of the “high-affinity” P-gp inhibitor [¹¹C]tariquidar was low in wild-type, P-gp (*mdr1a*^{-/-}/*mdr1b*^{-/-}6), and Bcrp(*abcg2*⁶) knockout mice but was high in P-gp/Bcrp (*mdr1a*^{-/-}/*mdr1b*^{-/-}/

Table 2. Calculated Values of Receptor Density for Various Efflux Transporters Expressed in Human, Monkey, and Mouse Brains^a

gene	protein	human		monkey		mouse	
		protein conc. (fmol/ μ g)	calculated B_{max} (nM)	protein conc. (fmol/ μ g)	calculated B_{max} (nM)	protein conc. (fmol/ μ g)	calculated B_{max} (nM)
ABC Transporters							
ABCA2		2.86	0.61	NR		ULQ	
ABCA8		1.21	0.26	NR		ULQ	
ABCB1	P-gp	6.06	1.28	4.71	1.00	14.1	2.99
ABCC4	Mrp4	0.195	0.04	0.286	0.06	1.59	0.34
ABCG2	Bcrp	4.07	0.86	7.10	1.51	2.20	0.47
SLC Transporters							
SLC1A3	EAAT1	24.5	5.19	NR		NR	
SLC2A1	GLUT1	139	29.47	129	27.35	90.0	19.08
SLC2A3	GLUT3	4.40	0.93	1.22	0.26	ULQ	
SLC3A2	4F2hc	3.47	0.74	NR		16.4	3.48
SLC6A12	BGT1	3.16	0.67	NR		NR	
SLC7A1	CAT1	1.13	0.24	NR		NR	
SLC7A5	LAT1	0.431	0.09	ULQ		2.19	0.46
SLC16A1	MCT1	2.27	0.48	0.834	0.18	23.7	5.02
SLC19A1	RFC	0.763	0.16	NR		NR	
SLC29A1	ENT1	0.568	0.12	0.541	0.11	0.985	0.21
Receptors							
INSR	insulin receptor	1.09	0.23	1.52	0.32	1.16	0.25
LRP1	Lrp1	1.51	0.32	1.29	0.27	1.07	0.23
TfR1	transferrin receptor	2.34	0.50	NR		5.84	1.24

^aABCG2/BCRP values are half that reported in Uchida and colleagues,²⁹ to account for the homodimerization of protein product to form a functional unit. ULQ = Under limit quantification. NR = Gene not reported/examined.

*abcg2*⁶) triple knockout mice.^{15,20} Tariquidar is a substrate for BCRP,¹² which explains its low uptake in wild-type and P-gp knockout mice. However, one would have expected higher uptake in Bcrp knockout mice because P-gp is still expressed in brain capillaries and can bind to [¹¹C]tariquidar. Brain uptake of other radiolabeled inhibitors followed a similar pattern in the four strains of mice.^{16,17,21,22}

Although extensive work has been done on P-gp inhibitors, only one putative BCRP inhibitor has been radiolabeled and tested in animals. The brain uptake of this ¹¹C-labeled compound (chemical name [¹¹C]methyl 4-((4-(2-(6,7-dimethoxy-1,2,3,4-tetrahydroisoquinolin-2-yl)ethyl)phenyl)amino-carbonyl)-2-(quinoline-2-carboxylamino)benzoate²³) in wild-type mice was high but was even higher in P-gp and P-gp/BCRP knockout mice, similar to results obtained with most of the P-gp inhibitors.²³

Among these eight reported ligands, only one inhibitor showed a different uptake profile. The P-gp inhibitor [¹¹C]-1 (chemical name 6,7-dimethoxy-2-{3-[4-methoxy-3,4-dihydro-2H naphthalene-(1E)-ylidene]-propyl}-1,2,3,4-tetrahydro-isoquinoline¹⁹) had a high brain uptake (>1.0 SUV) in rats at baseline conditions and a 30% reduced uptake after blockade of transporters.¹⁹ While these results are what one might expect from a PET study measuring efflux transporter density, they should be interpreted cautiously. The inhibitor [¹¹C]-1 is approximately 2 orders of magnitude less potent than tariquidar and elacridar²⁴ and may not, therefore, have the affinity required to specifically measure the density of P-gp at the blood–brain barrier (see discussion below).

■ TWO FACTORS AFFECT BRAIN SIGNAL IN PET STUDIES OF P-GP DENSITY

Low Binding Potential of Efflux Transporters. Even after blockade or genetic knockout of transporters, the raw values of brain uptake for most of the radiolabeled inhibitors are still lower (<1.8 standardized uptake value, SUV, Table 1) than those typically achieved with PET radioligands that bind to a specific receptor in the brain.²⁵ The fact that little or no brain signal was observed in conditions where P-gp is expressed and its density should be measurable suggests that either the density of P-gp in the whole brain (B_{max}) is not sufficient to allow visualization by PET or that the affinity ($1/K_D$) of the inhibitor is not high enough. In other words, while an inhibitor may bind to P-gp at the blood–brain barrier, binding in the *whole brain* is not detectable by PET because the binding potential (B_{max}/K_D) of the *whole brain* is too low. For a radioligand to have measurable brain uptake, the B_{max} should exceed the K_D of the ligand [A value of >5 for binding potential (B_{max}/K_D) is generally recommended to achieve measurable brain uptake; however, the field lacks consensus on this value]: if a binding site has nanomolar concentrations *in vivo*, then the radioligand should ideally have subnanomolar affinity.²⁶ What, then, is the binding potential for P-gp and a high-affinity inhibitor (e.g., tariquidar) in the whole brain?

Estimation of Efflux Transporter Density in the Whole Brain (B_{max}). To calculate the binding potential, an estimate of P-gp density in the whole brain (B_{max}) is required. Although the affinities of radiolabeled inhibitors for P-gp have been experimentally determined, the B_{max} has not [reports have been published on P-gp expression in cells of the brain parenchyma expressing P-gp (particularly during neuroinflammation) and in infiltrating lymphocytes]. However, for the purposes of this discussion we will assume that P-gp expression in

the brain occurs in the brain capillary endothelial cells only. Ordinarily, *in vitro* studies with brain homogenate are used to determine an approximate B_{\max} value,⁹ but the high lipophilicity of the P-gp inhibitors (e.g., clog P tariquidar = 6)²⁷ has made it difficult to estimate this value using this method. Instead, we use the values published recently by Terasaki and co-workers, who measured the expression of transporters in isolated brain capillary endothelial cells using quantitative liquid chromatography-tandem mass spectrometry. This method allows for measurement of protein levels, given as fmol/ μ g of cellular protein in endothelial cells isolated from brain capillaries of mice,²⁸ monkeys,²⁹ and humans³⁰ (summarized in Table 2).

From these studies, we know the concentration of transporters in human brain capillary endothelial cells, but not in the whole brain, which is necessary to calculate B_{\max} . Therefore, the calculation of the concentration of a protein expressed in capillary endothelial cells in the whole brain is critically reliant on knowledge of the density of brain capillary endothelial cells as a proportion of total brain tissue. This is distinct from the total brain capillary volume, which is much higher, as it includes blood volume. Blood volume in the brain is reported to be approximately 5% of total brain volume,^{31,32} but the capillary volume is significantly lower. A three-dimensional reconstruction of brain capillaries from frozen serial sections of feline temporoparietal Suprasylvian–Gyrus revealed an average capillary diameter of $4.68 \pm 0.92 \mu\text{m}$, total capillary length of $42.55 \text{ cm}/\text{mm}^2$ of brain tissue, and a capillary volume of 2.8%.³³

Yet there is surprisingly little experimental data on the volume occupied by endothelial cells in the brain. The principal values cited come from Pardridge,³⁴ who stated that, “Since the brain capillary endothelial cell volume is only $1 \mu\text{L}/\text{g}$ brain, the endothelial volume in brain is only 0.2% of the total cell volume in brain.” In an earlier report, Pardridge estimated that endothelial cell volume is $0.8 \mu\text{L}$ per g of brain, given a capillary volume of 1% of total brain volume, and that endothelial cells occupy one-tenth of the total capillary volume (Figure 1).³⁵

Is there experimental support for these approximations? The most useful data appears to come from Hicks and colleagues, who assessed the cross-sectional area of capillary components (basement membrane, endothelial cell, lumen, and pericyte) in the hippocampus and frontal cortex of rats of 3, 9, and 24 months of age.³⁶ Assessment of area was achieved by producing large photographic copies of each electron microscope image, cutting out the components, and weighing the pieces to calculate area. The percentage of area composed of endothelial cells in the frontal cortex was 12% and in the hippocampus was 11% (average basement membrane 4%, lumen 80%, and pericyte 4%). Given an experimental representative brain capillary volume of 2%, and an experimental representative endothelial cell volume that is 10% of the total capillary volume, brain capillary endothelial cell content is indeed estimated at 0.2% of brain volume.

Using the numbers from previous studies, we estimate that the B_{\max} of P-gp in the whole human brain is 1.3 nM (see Appendix A for detailed calculations). The method employed by Terasaki and colleagues to measure the expression of transporter protein did not differentiate between functional transporter at the luminal membrane and internalized transporter; as such, B_{\max} at the luminal membrane may be slightly lower (as noted earlier, inhibitors may bind both pools of P-gp). We have determined the B_{\max} values for other brain capillary transporters in a similar fashion (Table 2). It is notable that only two solute carrier transporters demonstrate higher expression in human brain

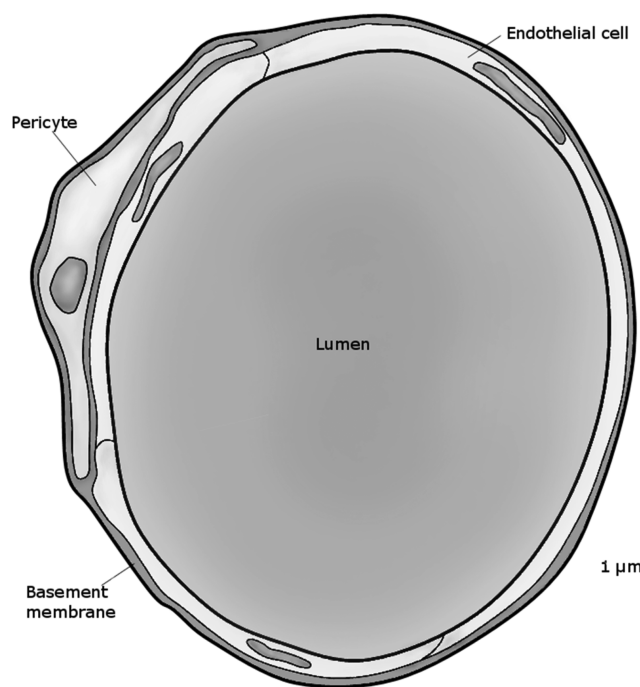


Figure 1. Diagram of cross-section from a rat brain capillary demonstrating that endothelial cells constitute a small percentage of the total capillary volume. The diagram was generated from electron micrograph published by Hicks and colleagues.³⁶ The scale bar represents $1 \mu\text{m}$.

endothelial cells than P-gp. They are associated with energy supply to the brain (glucose transporter 1, Glut1, *SLC2A1*, calculated brain concentration 29.5 nM) and glutamate supply (glutamate aspartate transporter, Eaat1, *SLC1A3*, calculated concentration 5.2 nM). While PET functional studies of Glut1 have been reported, and it is expressed only in brain endothelial cells,³⁷ no PET binding studies exist in the literature for this transporter.

Binding Potential (B_{\max}/K_D) of P-gp and “High-Affinity” Inhibitors. Using the B_{\max} value mentioned above for P-gp (1.3 nM) and reported K_D values for various P-gp inhibitors, we calculate that B_{\max}/K_D values range from 0.004 to 0.470 (Table 3). These values are well below the B_{\max}/K_D cutoff value of >5 – 10 recommended for a useful PET radioligand.²⁶ Although a similar mathematical approach was described in the literature, previous calculations used a vascular volume of 5% rather than a capillary density of 0.2%,¹⁵ concluding that the B_{\max}/K_D (i.e., the binding potential) for tariquidar, for instance, is 15, which would

Table 3. Calculated Values of Binding Potential (B_{\max}/K_D)^a for Various P-gp Inhibitors

inhibitor	K_D^b (nM)	species used for cell assay	reference	calculated B_{\max}/K_D for P-gp
cyclosporin A	300	hamster	42	0.004
elacridar	2.7	human	43	0.474
tariquidar	5.1	hamster	14	0.251
valsopodar	80	hamster	42	0.016
zosuquidar	55	hamster	42	0.023

^a B_{\max} = concentration of binding sites. K_D = equilibrium dissociation constant, where affinity of the ligand for the target is defined as $1/K_D$.
^bThe K_D value for the P-gp inhibitor, laniquidar, has not been reported.

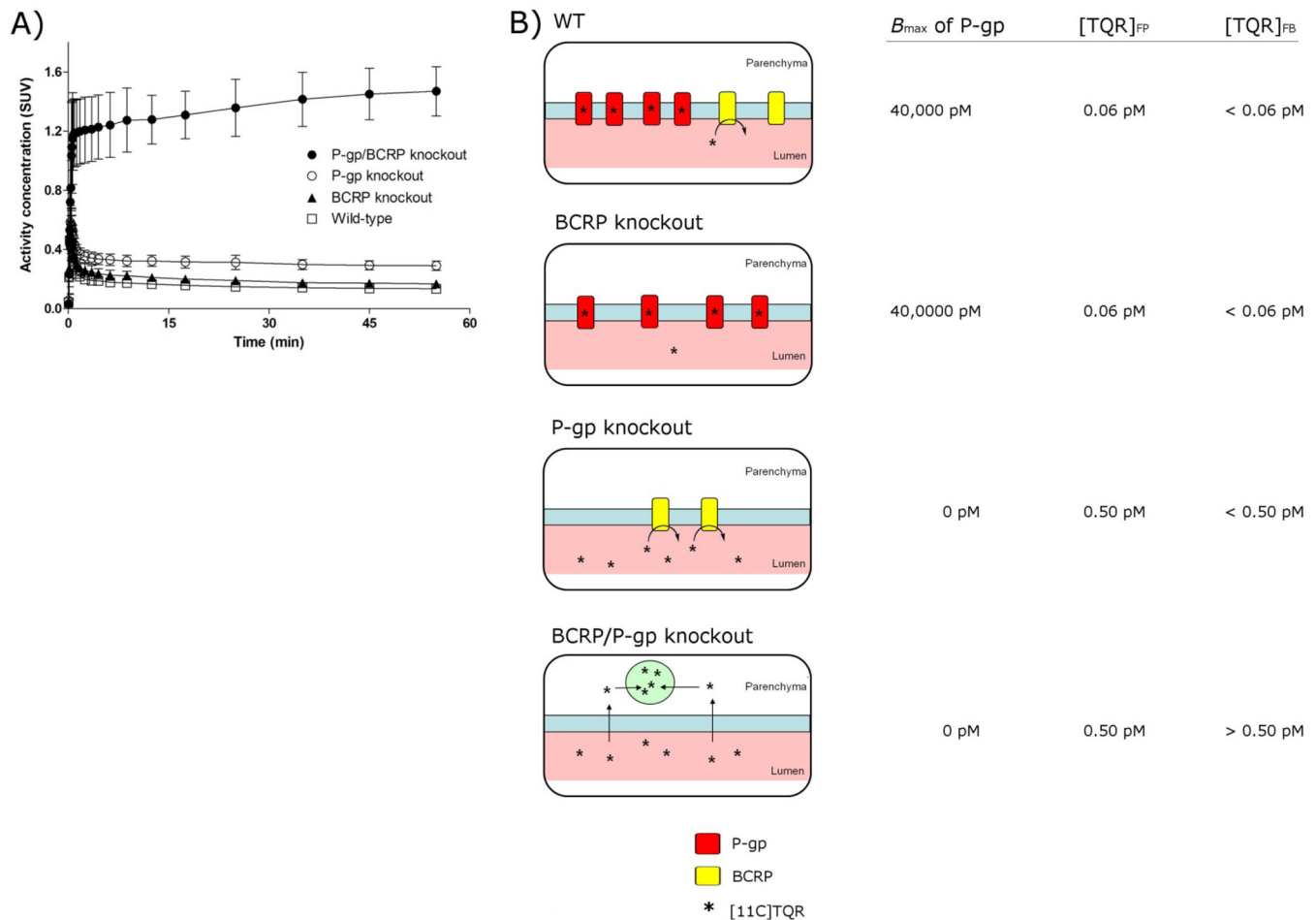


Figure 2. The high, localized density of P-glycoprotein (P-gp) may transiently reduce the free plasma concentration of $[^{11}C]$ tariquidar in brain capillaries, which may subsequently reduce the concentration of free radioligand in the brain. (A) Uptake of $[^{11}C]$ tariquidar, as measured by positron emission tomography (PET), is low in brains of wild-type and Bcrp knockout, 2-fold higher in P-gp knockout mice, and 9.3-fold higher in P-gp/Bcrp knockout mice. Modified with permission from data published by Langer and colleagues¹⁵ (2010). Copyright 2010 Elsevier. (B) Scheme demonstrating the potential interactions of radiolabeled inhibitor $[^{11}C]$ tariquidar (indicated by *) with transporters P-gp (red) and breast cancer resistance protein (Bcrp, yellow). The numbers to the right of each image are representative values for the density (B_{max}) of P-gp, free concentration of tariquidar in plasma ($[TQR]_{FP}$), and free concentration of tariquidar in brain ($[TQR]_{FB}$) for each mouse strain. The values were calculated assuming that the density of P-gp is 40 000 pM in the capillaries, and that tariquidar has a concentration of 1 nM in the capillary, a K_D of 5 nM, and a free fraction of 0.05 (meaning a free concentration of tariquidar of 0.50 pM). In wild-type and Bcrp knockout mice, for every one molecule of tariquidar that is free, eight molecules are bound to P-gp; this binding further decreases the free concentration of tariquidar in plasma to 0.06 pM. In P-gp knockout mice, the free concentration of tariquidar is not further reduced by high-affinity binding to P-gp, although overall parenchymal uptake is still low because the inhibitor is efficiently effluxed as a substrate of Bcrp. In P-gp/Bcrp knockout mice, the radiolabeled molecule is taken up in the brain and trapped (probably by lysosomal trapping⁷).

allow for obtaining a sufficiently high in vivo signal with radiolabeled tariquidar (subsequently corrected³⁸).

There are clearly limitations to our calculations because they are based on experimentally determined values derived from a range of species: rabbit (brain capillary density), rat (capillary cross sections), human (capillary transporter density and brain protein density), and hamster (inhibitors' K_D for P-gp). Nevertheless, it is clear that the concentration of P-gp in the whole brain is very low (<1 nM). Given such a low B_{max} for P-gp in the whole brain, the affinity of tariquidar and other "high-affinity" inhibitors needs to be at least an order of magnitude higher (picomolar) to allow PET imaging. For example, based on a calculated B_{max} of 1.3 nM for P-gp in the whole brain and a binding potential threshold of 5 for imaging, a K_D of 260 pM (or lower in value) would need to be achieved before imaging the density of P-gp is possible.

High, Localized Transporter Density. Although conventional PET studies of receptor density in the brain require brain penetration of a radioligand,²⁵ PET studies of transporter density do not, as the target (i.e., efflux transporters) is located within capillary walls. At this location, which is exposed to the plasma compartment, efflux transporters can have a direct effect on the free concentration of radioligand. Because only free radioligand can bind to a target, we speculate that this effect on drug disposition is more likely to affect tracer concentrations of drug than pharmacological doses.

We propose that the local density of P-gp in the endothelial cells is so high that it transiently binds a high percentage of radiolabeled inhibitor, thereby lowering the free concentration in the capillary such that a negligible amount would enter the brain. If all P-gp is concentrated in the capillary volume, then its concentration (B_{max}) in the capillary space is 40 nM. To illustrate the effect of high, localized density on free ligand concentration,

we used the Michaelis–Menten equation to calculate the bound–free ratio and receptor occupancy for the inhibitor tariquidar (see Appendix B). As the concentration of free radioligand decreases, the bound–free ratio increases to a maximum of eight. In other words, for each free molecule of tariquidar in the brain capillary, eight molecules are bound to P-gp. Despite this high bound–free ratio, the receptor occupancy at this concentration (0.001 nM) is very low (0.02%).

What would be the predicted receptor occupancy with tracer doses of [¹¹C]tariquidar in PET? Radioligands that are too lipophilic are highly bound to plasma proteins, which would dramatically reduce the free plasma concentration of radioligand.³⁹ Like elacridar and laniquidar, tariquidar is a highly lipophilic compound (clog *P* = 6)²⁷ that is highly bound to plasma proteins: we have observed the free plasma concentration of [¹¹C]tariquidar to be 0.05% (i.e., 99.95% protein binding). In other words, if the concentration of tariquidar is 1 nM in the vascular space, then the free plasma concentration of tariquidar is 0.5 pM. Thus, in a capillary where the local concentration of P-gp is 40 000 pM, the total bound P-gp in this situation is 4 pM or 0.01%—a negligible part of total radioactivity (1 nM).

Based on the above calculations, we hypothesize that the binding of [¹¹C]tariquidar to P-gp is so effective that it lowers the concentration of free radioligand in plasma, which then passively affects the concentration of free radioligand in the brain. One limitation of this analysis is that it is based on theoretical data and approximations and thus may not represent the entire *in vivo* situation. However, our hypothesis that high, localized density of P-gp contributes to the low brain signal in PET is supported by the observation that P-gp knockout mice had slightly higher brain signal from [¹¹C]tariquidar than wild-type mice did¹⁵ (Figure 2). This result would be predicted because P-gp knockout mice lack the receptor that transiently decreases the free concentration of [¹¹C]tariquidar in capillary plasma; however, parenchymal uptake is still low because tariquidar is effluxed as a substrate of BCRP. Taken together, the above calculations and the observations in mice support a hypothesis, not previously discussed, that the microenvironment of the capillary affects the low brain signal obtained from radiolabeled inhibitors in PET studies of P-gp density.

CONCLUSIONS

Imaging the density of efflux transporters, such as P-gp, in the blood–brain barrier using high-affinity inhibitors and PET presents a particular challenge. Based on our calculations, we postulate that, while P-gp is highly expressed in brain capillary endothelial cells, the endothelial cells themselves are present in a low but relatively uniform density throughout the brain. Compared with a small region of the brain with locally high expression of a protein, which can be quantified by PET imaging, the very low density of P-gp in the brain, high protein binding, and locally reduced plasma concentrations will require an imaging agent with a significantly higher affinity for P-gp. More generally, locally high concentrations of transporters and receptors in brain endothelial cells do not appear amenable to imaging due to the vast dilution of endothelial capillary cells in the brain. The development of radiotracers with picomolar affinity for targets will be needed to develop diagnostic tools capable of providing insight into an ever-increasing list of pathophysiological associated with dysfunction at the blood–brain barrier.

APPENDIX A: CALCULATION OF B_{MAX} (MOL/L) OF P-GP IN THE WHOLE BRAIN

Values are derived from values found in the literature that can be generally applied to determine the B_{max} of other proteins in brain endothelial cells. Four values are necessary:

- The human brain endothelial cell P-gp expression, which is 6.06 fmol/ μg protein (6.06 nmol/g);²⁸
- The protein content of the human brain, which is reported as $\sim 10\%$ of total wet weight (i.e., 100 mg protein/g brain), and fairly uniform across all regions;⁴⁰
- The density of the human brain, which is 1060 g/L;⁴¹ and
- The aforementioned endothelial cell density in the brain of 0.2%.

A concentration of 6.06 nmol P-gp/g of protein (a) is 0.606 nmol P-gp/g brain (10-fold dilution of protein content in cells, value b), which consequently gives a P-gp concentration of 642 nmol/L (using value c for density of brain). Diluting for endothelial cells as a component of total brain (0.2%, value d) gives a final estimated concentration of P-gp in the brain of 1.3 nM.

APPENDIX B: CALCULATION OF BOUND–FREE RATIO AND RECEPTOR OCCUPANCY FOR TARIQUIDAR AND P-GP IN BRAIN CAPILLARIES

Equilibrium Michaelis–Menten:

$$\frac{B}{F} = \frac{B_{\text{max}}}{K_D + F} \quad (1)$$

If $F \ll K_D$:

$$\frac{B}{F} = \frac{B_{\text{max}}}{K_D} = B_{\text{max}} \times \text{affinity} \quad (2)$$

where B = concentration of bound radiotracer; F = concentration of free radiotracer; B_{max} = concentration of receptor target; K_D = dissociation constant of radiotracer.

The equilibrium Michaelis–Menten eq 1 is used to determine the bound (B) concentration of radiotracer given that the other variables are known. When the free (F) concentration is much lower than the K_D for the radiotracer ($F \ll K_D$), F can be removed (eq 2).

The receptor occupancy (RO), the percentage of receptor bound by radiotracer, can subsequently be calculated using eq 3:

$$\text{RO} = \frac{B_{\text{max}}}{B_{\text{max}}} = \frac{F}{K_D + F} \quad (3)$$

Given that in capillaries the B_{max} for P-gp and K_D for tariquidar are known, a range of free tariquidar concentrations (F) can be used to compute theoretical bound (B) concentration, bound–free ratio (B/F), and receptor occupancy (RO) of the radiotracer (see Table A1).

Table A1

B_{max} (nM)	F (nM)	B (nM)	B/F	RO
40	10	26.67	2.7	66.67%
	1	6.67	6.7	16.67%
K_D (nM)	0.1	0.78	7.8	1.96%
	0.01	0.08	8.0	0.20%
	0.001	0.01	8.0	0.02%

AUTHOR INFORMATION

Corresponding Author

*National Institute of Mental Health, 10 Center Drive, Rm B1D43, Bethesda, Maryland 20892-1026, United States. Fax: +1 301 480 3610. Tel.: +1 301 594 1368. E-mail: robert.innis@nih.gov.

Notes

The authors declare no competing financial interest.

ACKNOWLEDGMENTS

This research was supported by the Intramural Research Programs of the National Institute of Mental Health (Project Nos. Z01-MH-002852-04 and MH002793-09) and the National Cancer Institute (Project no. Z01-BC-005598). Oliver Langer's studies are funded by the Austrian Science Fund (FWF) project "Transmembrane Transporters in Health and Disease" (SFB F35) and by the European Community's Seventh Framework Programme (FP7/2007-2013) under grant agreement number 201380 ("EURIPIDES"). We thank George Leiman for editorial assistance.

REFERENCES

(1) Kannan, P.; John, C.; Zoghbi, S. S.; Halldin, C.; Gottesman, M. M.; Innis, R. B.; Hall, M. D. Imaging the function of P-glycoprotein with radiotracers: pharmacokinetics and in vivo applications. *Clin. Pharm. Ther.* **2009**, *86* (4), 368–77.

(2) Cooray, H. C.; Blackmore, C. G.; Maskell, L.; Barrand, M. A. Localisation of breast cancer resistance protein in microvessel endothelium of human brain. *Neuroreport* **2002**, *13* (16), 2059–63.

(3) Graff, C. L.; Pollack, G. M. Drug transport at the blood–brain barrier and the choroid plexus. *Curr. Drug Metab.* **2004**, *5* (1), 95–108.

(4) Dombrowski, S. M.; Desai, S. Y.; Marroni, M.; Cucullo, L.; Goodrich, K.; Bingaman, W.; Mayberg, M. R.; Bengezi, L.; Janigro, D. Overexpression of multiple drug resistance genes in endothelial cells from patients with refractory epilepsy. *Epilepsia* **2001**, *42* (12), 1501–6.

(5) Loscher, W.; Potschka, H. Drug resistance in brain diseases and the role of drug efflux transporters. *Nat. Rev. Neurosci.* **2005**, *6* (8), 591–602.

(6) Phelps, M. *Molecular Imaging and Its Biological Applications*; Springer: New York, 2004.

(7) Kannan, P.; Brimacombe, K. R.; Kreisl, W. C.; Liow, J. S.; Zoghbi, S. S.; Telu, S.; Zhang, Y.; Pike, V. W.; Halldin, C.; Gottesman, M. M.; Innis, R. B.; Hall, M. D. Lysosomal trapping of a radiolabeled substrate of P-glycoprotein as a mechanism for signal amplification in PET. *Proc. Natl. Acad. Sci. U.S.A.* **2011**, *108* (6), 2593–8.

(8) Piwnica-Worms, D.; Sharma, V. Probing multidrug resistance P-glycoprotein transporter activity with SPECT radiopharmaceuticals. *Curr. Top. Med. Chem.* **2010**, *10* (17), 1834–45.

(9) Innis, R. B.; Cunningham, V. J.; Delforge, J.; Fujita, M.; Gjedde, A.; Gunn, R. N.; Holden, J.; Houle, S.; Huang, S. C.; Ichise, M.; Iida, H.; Ito, H.; Kimura, Y.; Koeppe, R. A.; Knudsen, G. M.; Knuuti, J.; Lammertsma, A. A.; Laruelle, M.; Logan, J.; Maguire, R. P.; Mintun, M. A.; Morris, E. D.; Parsey, R.; Price, J. C.; Slifstein, M.; Sossi, V.; Suhara, T.; Votaw, J. R.; Wong, D. F.; Carson, R. E. Consensus nomenclature for in vivo imaging of reversibly binding radioligands. *J. Cereb. Blood Flow Metab.* **2007**, *27* (9), 1533–9.

(10) Ambudkar, S. V.; Dey, S.; Hrycyna, C. A.; Ramachandra, M.; Pastan, I.; Gottesman, M. M. Biochemical, cellular, and pharmacological aspects of the multidrug transporter. *Annu. Rev. Pharmacol. Toxicol.* **1999**, *39*, 361–98.

(11) Colabufo, N. A.; Berardi, F.; Perrone, M. G.; Capparelli, E.; Cantore, M.; Inglesse, C.; Perrone, R. Substrates, inhibitors and activators of P-glycoprotein: candidates for radiolabeling and imaging perspectives. *Curr. Top. Med. Chem.* **2010**, *10* (17), 1703–14.

(12) Kannan, P.; Telu, S.; Shukla, S.; Ambudkar, S. V.; Pike, V. W.; Halldin, C.; Gottesman, M. M.; Innis, R. B.; Hall, M. D. The "Specific" P-Glycoprotein Inhibitor Tariquidar Is Also a Substrate and an Inhibitor

for Breast Cancer Resistance Protein (BCRP/ABCG2). *ACS Chem. Neurosci.* **2011**, *2* (2), 82–9.

(13) Loo, T. W.; Bartlett, M. C.; Detty, M. R.; Clarke, D. M. The ATPase activity of the P-glycoprotein drug pump is highly activated when the N-terminal and central regions of the nucleotide-binding domains are linked closely together. *J. Biol. Chem.* **2012**, *287* (32), 26806–16.

(14) Martin, C.; Berridge, G.; Mistry, P.; Higgins, C.; Charlton, P.; Callaghan, R. The molecular interaction of the high affinity reversal agent XR9576 with P-glycoprotein. *Br. J. Pharmacol.* **1999**, *128* (2), 403–11.

(15) Bauer, F.; Kuntner, C.; Bankstahl, J. P.; Wanek, T.; Bankstahl, M.; Stanek, J.; Mairinger, S.; Dorner, B.; Loscher, W.; Muller, M.; Erker, T.; Langer, O. Synthesis and in vivo evaluation of [¹¹C]tariquidar, a positron emission tomography radiotracer based on a third-generation P-glycoprotein inhibitor. *Bioorg. Med. Chem.* **2010**, *18* (15), 5489–97.

(16) Dorner, B.; Kuntner, C.; Bankstahl, J. P.; Bankstahl, M.; Stanek, J.; Wanek, T.; Stundner, G.; Mairinger, S.; Loscher, W.; Muller, M.; Langer, O.; Erker, T. Synthesis and small-animal positron emission tomography evaluation of [¹¹C]-elacridar as a radiotracer to assess the distribution of P-glycoprotein at the blood–brain barrier. *J. Med. Chem.* **2009**, *52* (19), 6073–82.

(17) Dorner, B.; Kuntner, C.; Bankstahl, J. P.; Wanek, T.; Bankstahl, M.; Stanek, J.; Mullauer, J.; Bauer, F.; Mairinger, S.; Loscher, W.; Miller, D. W.; Chiba, P.; Muller, M.; Erker, T.; Langer, O. Radiosynthesis and in vivo evaluation of 1-[¹⁸F]fluoroelacridar as a positron emission tomography tracer for P-glycoprotein and breast cancer resistance protein. *Bioorg. Med. Chem.* **2011**, *19* (7), 2190–8.

(18) Luurtsema, G.; Schuit, R. C.; Klok, R. P.; Verbeek, J.; Leysen, J. E.; Lammertsma, A. A.; Windhorst, A. D. Evaluation of [¹¹C]laniquidar as a tracer of P-glycoprotein: radiosynthesis and biodistribution in rats. *Nucl. Med. Biol.* **2009**, *36* (6), 643–9.

(19) van Waarde, A.; Ramakrishnan, N. K.; Rybczynska, A. A.; Elsinga, P. H.; Berardi, F.; de Jong, J. R.; Kwizera, C.; Perrone, R.; Cantore, M.; Sijbesma, J. W.; Dierckx, R. A.; Colabufo, N. A. Synthesis and preclinical evaluation of novel PET probes for P-glycoprotein function and expression. *J. Med. Chem.* **2009**, *52* (14), 4524–32.

(20) Kawamura, K.; Konno, F.; Yui, J.; Yamasaki, T.; Hatori, A.; Yanamoto, K.; Wakizaka, H.; Takei, M.; Nengaki, N.; Fukumura, T.; Zhang, M. R. Synthesis and evaluation of [¹¹C]XR9576 to assess the function of drug efflux transporters using PET. *Ann. Nucl. Med.* **2010**, *24* (5), 403–12.

(21) Kawamura, K.; Yamasaki, T.; Konno, F.; Yui, J.; Hatori, A.; Yanamoto, K.; Wakizaka, H.; Ogawa, M.; Yoshida, Y.; Nengaki, N.; Fukumura, T.; Zhang, M. R. Synthesis and in vivo evaluation of (1)(8)F-fluoroethyl GF120918 and XR9576 as positron emission tomography probes for assessing the function of drug efflux transporters. *Bioorg. Med. Chem.* **2011**, *19* (2), 861–70.

(22) Kawamura, K.; Yamasaki, T.; Konno, F.; Yui, J.; Hatori, A.; Yanamoto, K.; Wakizaka, H.; Takei, M.; Kimura, Y.; Fukumura, T.; Zhang, M. R. Evaluation of limiting brain penetration related to P-glycoprotein and breast cancer resistance protein using [(11)C]-GF120918 by PET in mice. *Mol. Imaging Biol.* **2011**, *13* (1), 152–60.

(23) Mairinger, S.; Langer, O.; Kuntner, C.; Wanek, T.; Bankstahl, J. P.; Bankstahl, M.; Stanek, J.; Dorner, B.; Bauer, F.; Baumgartner, C.; Loscher, W.; Erker, T.; Muller, M. Synthesis and in vivo evaluation of the putative breast cancer resistance protein inhibitor [¹¹C]methyl 4-((4-(2-(6,7-dimethoxy-1,2,3,4-tetrahydroisoquinolin-2-yl)ethyl)phenyl)-amino-carbonyl)-2-(quinoline-2-carboxylamino)benzoate. *Nucl. Med. Biol.* **2010**, *37* (5), 637–44.

(24) Mairinger, S.; Wanek, T.; Kuntner, C.; Doenmez, Y.; Strommer, S.; Stanek, J.; Capparelli, E.; Chiba, P.; Muller, M.; Colabufo, N. A.; Langer, O. Synthesis and preclinical evaluation of the radiolabeled P-glycoprotein inhibitor [(11)C]MC113. *Nucl. Med. Biol.* **2012**, *39* (8), 1219–25.

(25) Halldin, C.; Gulyas, B.; Langer, O.; Farde, L. Brain radioligands—state of the art and new trends. *Q. J. Nucl. Med.* **2001**, *45* (2), 139–52.

(26) Eckelman, W. C.; Mathis, C. A. Targeting proteins in vivo: in vitro guidelines. *Nucl. Med. Biol.* **2006**, *33* (2), 161–4.

(27) Luurtsema, G.; Verbeek, G. L.; Lubberink, M.; Lammertsma, A. A.; Dierckx, R.; Elsinga, P.; Windhorst, A. D.; van Waarde, A. Carbon-11 labeled tracers for in vivo imaging P-glycoprotein function: kinetics, advantages and disadvantages. *Curr. Top. Med. Chem.* **2010**, *10* (17), 1820–33.

(28) Kamiie, J.; Ohtsuki, S.; Iwase, R.; Ohmine, K.; Katsukura, Y.; Yanai, K.; Sekine, Y.; Uchida, Y.; Ito, S.; Terasaki, T. Quantitative atlas of membrane transporter proteins: development and application of a highly sensitive simultaneous LC/MS/MS method combined with novel in-silico peptide selection criteria. *Pharm. Res.* **2008**, *25* (6), 1469–83.

(29) Ito, K.; Uchida, Y.; Ohtsuki, S.; Aizawa, S.; Kawakami, H.; Katsukura, Y.; Kamiie, J.; Terasaki, T. Quantitative membrane protein expression at the blood–brain barrier of adult and younger cynomolgus monkeys. *J. Pharm. Sci.* **2011**, *100* (9), 3939–50.

(30) Uchida, Y.; Ohtsuki, S.; Katsukura, Y.; Ikeda, C.; Suzuki, T.; Kamiie, J.; Terasaki, T. Quantitative targeted absolute proteomics of human blood–brain barrier transporters and receptors. *J. Neurochem.* **2011**, *117* (2), 333–45.

(31) Larsson, H. B.; Courivaud, F.; Rostrup, E.; Hansen, A. E. Measurement of brain perfusion, blood volume, and blood–brain barrier permeability, using dynamic contrast-enhanced T(1)-weighted MRI at 3 T. *Magn. Reson. Med.* **2009**, *62* (5), 1270–81.

(32) Phelps, M. E.; Huang, S. C.; Hoffman, E. J.; Kuhl, D. E. Validation of tomographic measurement of cerebral blood volume with C-11-labeled carboxyhemoglobin. *J. Nucl. Med.* **1979**, *20* (4), 328–34.

(33) Wiederhold, K. H.; Bielser, W., Jr.; Schulz, U.; Veteau, M. J.; Hunziker, O. Three-dimensional reconstruction of brain capillaries from frozen serial sections. *Microvasc. Res.* **1976**, *11* (2), 175–80.

(34) Pardridge, W. M. Blood-brain barrier biology and methodology. *J. Neurovirol.* **1999**, *5* (6), 556–69.

(35) Pardridge, W. *Peptide Drug Delivery to the Brain*; Raven Press: New York, 1991; p 357.

(36) Hicks, P.; Rolsten, C.; Brizzee, D.; Samorajski, T. Age-related changes in rat brain capillaries. *Neurobiol. Aging* **1983**, *4* (1), 69–75.

(37) Pardridge, W. M.; Boado, R. J.; Farrell, C. R. Brain-type glucose transporter (GLUT-1) is selectively localized to the blood–brain barrier. Studies with quantitative western blotting and in situ hybridization. *J. Biol. Chem.* **1990**, *265* (29), 18035–40.

(38) Mairinger, S.; Erker, T.; Muller, M.; Langer, O. PET and SPECT radiotracers to assess function and expression of ABC transporters in vivo. *Curr. Drug Metab.* **2011**, *12* (8), 774–92.

(39) Zoghbi, S. S.; Anderson, K. B.; Jenko, K. J.; Luckenbaugh, D. A.; Innis, R. B.; Pike, V. W. On quantitative relationships between drug-like compound lipophilicity and plasma free fraction in monkey and human. *J. Pharmaceut. Sci.* **2012**, *101* (3), 1028–39.

(40) Banay-Schwartz, M.; Kenessey, A.; DeGuzman, T.; Lajtha, A.; Palkovits, M. Protein content of various regions of rat brain and adult and aging human brain. *Age* **1992**, *15* (2), 51–54.

(41) Witelson, S. F.; Beresh, H.; Kigar, D. L. Intelligence and brain size in 100 postmortem brains: sex, lateralization and age factors. *Brain* **2006**, *129* (Pt 2), 386–98.

(42) Melchior, D. L.; Sharom, F. J.; Evers, R.; Wright, G. E.; Chu, J. W.; Wright, S. E.; Chu, X.; Yabut, J. Determining P-glycoprotein-drug interactions: evaluation of reconstituted P-glycoprotein in a liposomal system and LLC-MDR1 polarized cell monolayers. *J. Pharmacol. Toxicol. Meth.* **2012**, *65* (2), 64–74.

(43) Ferry, D. R.; Russell, M. A.; Kerr, D. J.; Correa, I. D.; Prakash, S. R. [³H]-GG918 (GF120918) binds with positive co-operativity to human P-glycoprotein with a nM dissociation constant. *Proc. Am. Assoc. Cancer Res.* **1996**, *37*, 2246.